

Study on Corrosion Properties and Microstructure of PEO Coatings Formed on AZ31 Mg Alloy

Yuanji. Shi^{1,*}, Junwan Li², Hongjun Wang¹, Hongchun Teng¹

¹ Department of Mechanical Engineering, Nanjing Institute of Industry Technology, Nanjing Jiangsu 210046, China;

² School of Materials Science and Engineering, Shanghai University, Shanghai 200072, China.

*E-mail: yuanji_shi@hotmail.com

Received: 6 February 2020 / Accepted: 18 March 2020 / Published: 10 May 2020

Plasma electrolytic oxidation(PEO) coatings were fabricated on AZ31 Mg alloy in phosphate-silicate based electrolyte with additive K_2ZrF_6 . The physical and chemical properties of the coatings were studied by SEM, AFM, XRD, XPS, potentiodynamic polarization and electrochemical impedance spectroscopy (EIS) test. The attained results showed that the thickness of the PEO coatings linearly increased with the increment treatment time. Besides, the micropores and corrosion resistance of the coatings varied with the PEO treatment time. The XRD presentation proved that the coatings were mainly composed of MgO, MgF₂, MgSiO₃ and ZrO₂. Moreover, the EIS results matched well with the potentiodynamic polarization test results.

Keywords: AZ31 Mg alloy; Corrosion; Potentiodynamic polarization; PEO Coatings; EIS

1. INTRODUCTION

In the recent years, the magnesium and their alloys has been widely used because of their easy-formation ability, good micro-hardness and deformation ability [1,2]. Unfortunately, a fatal shortcoming, that is the high possibility to be corroded, which greatly obstruct their applications [3]. Specially in some extreme environment, the magnesium alloys were very easy to be corroded and then become invalid.

Plasma electrolytic oxidation(PEO) as a new surface treatment technology, has gained so many attentions from the outside world since this century. However, as a new technology, it can only produce ceramic coatings on aluminum, magnesium, titanium and their alloys. On the other hand, it is a quite simple technology, that is, the coatings can be formed in the electrolyte with high voltages on these valve metals [4-9]. The detailed PEO treatment process can be illustrated as following: At first, there emerges some small bubbles on the surface of the specimen. After a short while, some sporadic sparks appears

with the bubbles. As the treatment time continues, some small bubbles becomes big and many big air pockets bubbles up. Almost on the same time, so many sparks gathered into the same area and becomes arc. And with the treatment process becomes intense, the big bubbles and arcs continuously appears on the surface of the samples. The whole process were happened under the high temperature. In the end, the ceramic coatings were fabricated on the surface of the specimens. And owing to the ceramic coatings, the coatings can provide superior protection to the specimens and prevent the specimen from corrosion. Hence, PEO has been widely used to fabricate ceramic coatings on the magnesium alloys which is of high sensitivity to be corroded [10-13].

Recently, there appears so many investigations of magnesium alloys. However, most of the investigations are very superficial. In this paper, the PEO coatings were thoroughly investigated by AFM. On the other hand, the electrochemical methods were used to investigate the corrosion behavior of the coatings.

2. EXPERIMENT DETAIL

2.1. PEO preparation

Specimens of AZ31 Mg alloy with size of 20 mm × 20 mm × 3 mm were cut from casting material. Its composition is showed in Table 1. Before treatment, all the specimens were mechanically polished with metallographic abrasive paper up to 1000# and cleaned, then dried. The treatment electrolyte consisted of 10 g/l of Na₃PO₄ and 10 g/l of Na₂SiO₃ and 8 g/l C₃H₈O₃ with 8 g/l additive K₂ZrF₆. In the treatment process, the specimen and barrel were selected as anode and cathode, respectively. The PEO specimens were prepared under different treatment time. The exact parameters are showed in Table 2.

Table 1 Composition of the substrate alloy in this study.

| Element | Al | Zn | Mn | Si | Ca | Cu | Fe | Ni | Mg |
|---------|---------|---------|---------|------|------|------|-------|-------|------|
| wt.% | 2.5-3.5 | 0.6-1.4 | 0.2-1.0 | 0.08 | 0.04 | 0.01 | 0.003 | 0.001 | Bal. |

Table 2. Parameters used in this study.

| Treatment time (Min) | Voltage (V) | Frequency (Hz) | Duty cycle |
|----------------------|-------------|----------------|------------|
| 10 | 420 | 400 | 4% |
| 20 | 420 | 400 | 4% |
| 30 | 420 | 400 | 4% |
| 40 | 420 | 400 | 4% |

2.2. Characterization of coatings

The surface and cross-section morphology of the PEO coatings were observed using scanning electron microscopy (SEM, JSM-6360LA). To further analyze the structure of coatings, atomic force

microscope (AFM, Nanoman VS) in air with a silicon tip of 10 nm radius in contact mode was employed to study the surface profile of coatings. The coating thickness and roughness of the samples were evaluated by SEM inspection and surface profilometer, respectively. X-ray diffraction (XRD) was carried out with Digaku D/max-2500 equipped with Cu K α radiation to detect the composition of the coatings. The measured range was between 2θ values of 20° and 80° with the X-ray generator settings were 45 kV and 40 mA, respectively. The scanning rate was $1^\circ/\text{min}$ with a step length of 0.02° . To further detect the composition of the coatings, the coating surface were etched for 1 min by argon-ion-beam and then analyzed by X-ray photoelectron spectroscopy (XPS, ESCALAB 250, Thermo VG Scientific). The C 1s signal was set at 284.6 eV [14].

2.3. Corrosion evaluation

The electrochemical experiment was performed in 3.5 wt.% NaCl solution using CorrTest AC potentiostat/frequency response analyzer system to evaluate the corrosion resistance of the PEO coatings. A corrosion cell with three-electrode-cell system: a weight-saving platinum electrode auxiliary electrode, a saturated calomel electrode (SCE) reference electrode and the specimens selected as working electrode were used in this study.

Prior to open circuit potentials (OCPs) experiment, an approximately 30 min wait time needs to be prepared for the specimens. Electrochemical impedance spectroscopy (EIS) studies were carried out at OCP with a perturbation amplitude signal of 10 mV within a frequency range of 105 Hz to 10-1 Hz. Besides, the PEO coated specimens were immersed in the salt electrolyte with 140 h for corrosion testing.

3. RESULTS AND DISCUSSION

3.1. Thickness and roughness

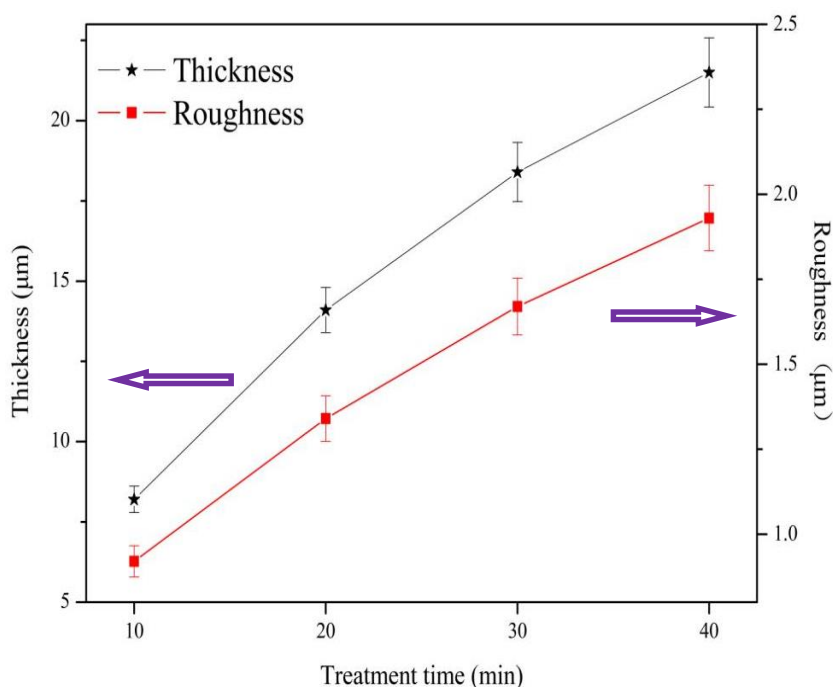


Figure 1. The thickness variation of PEO coatings in this study.

The thickness and roughness of PEO coatings formed on AZ31 Mg alloy in the electrolyte are showed in Fig.1. Clearly, it can be seen that the thickness and roughness increased with the increment of the treatment time (See Fig.1). Besides, the coating thickness was increased linearly with the reaction time approximately. Through the line fitting of the thickness vs. time, with the result shown in formula:

$$\text{Thickness } (\mu\text{m}) \approx 4.5 + 0.42 \times \text{Time (min)} \quad (1)$$

The growth rate of the PEO coating was $0.42 \mu\text{m}/\text{min}$. The coating formed in the electrolyte at the voltage of 420 V presented the thickest thickness with the treatment time of 40 min. In the initial of the PEO process, the coating accumulates at the magnesium/oxide/electrolyte interfaces, which led to the migration of $\text{O}^{2-}/\text{OH}^-$, similar to the titanium [15]. With the treatment time prolonged, the coating becomes thicker. Finally, the PEO reaction becomes stable and the coating grows relatively slow. At the same way, the roughness of the coating with the longest treatment time was of the highest value. On the other hand, with the treatment time increased, the pore sizes becomes larger, and the surface roughness increased.

3.2. Microstructure

Surface images of the PEO coatings formed in the K_2ZrF_6 -containing electrolyte are showed in Fig.2. The coatings are full of pores because the treatment was happened under the temperature of 104 K likely [16].

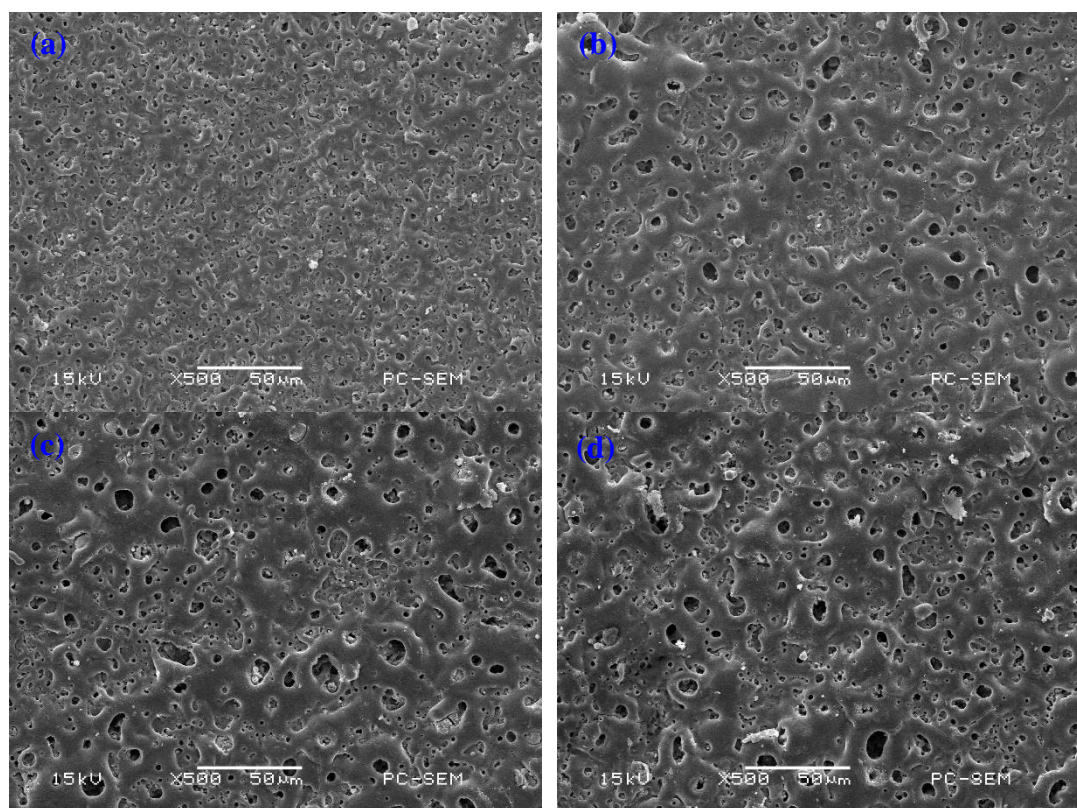


Figure 2. Surface images of PEO coatings with the treatment time: (a) 10 min, (b) 20 min, (c) 30 min, (d) 40 min, respectively.

When the treatment time is 10 min, there only exists some small pores on its surface (Fig.2a). But, with the treatment time increased, the pores decreased on numbers and increased on size. Specially, when the treatment time increased to 40 min, some large pores emerge (Fig.2d).

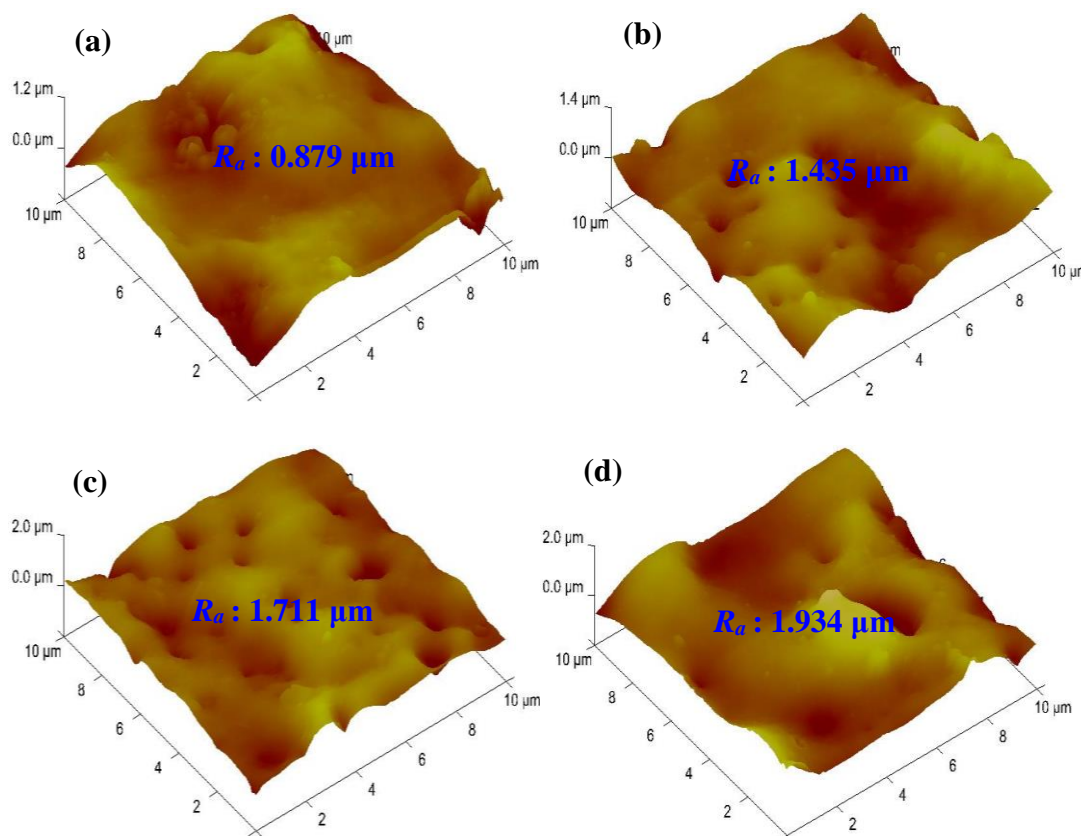


Figure 3. AFM surface topography of PEO coatings with the treatment time: (a) 10 min, (b) 20 min, (c) 30 min, (d) 40 min, respectively.

To observe the three-dimensional morphology of the coating, Fig.3 shows the 3D image of the coatings observed by the AFM. Generally, the height of the surface morphology that reflected by the AFM indicated the surface roughness of the coating on some extent. It means that if the value is large, the corresponding coating is of big roughness either. From the figure, it is showed that the value on the left top of the coating increased as the time lasted. Besides, to confirm the AFM results, it can be found that the surface roughness of the coating measured by the surface profilometre increased with the increasing treatment time (See Fig.1). The pattern is consistent with the AFM measured results. The coating with the longest treatment time showed the highest mean surface roughness (R_a , ~1.934 μm).

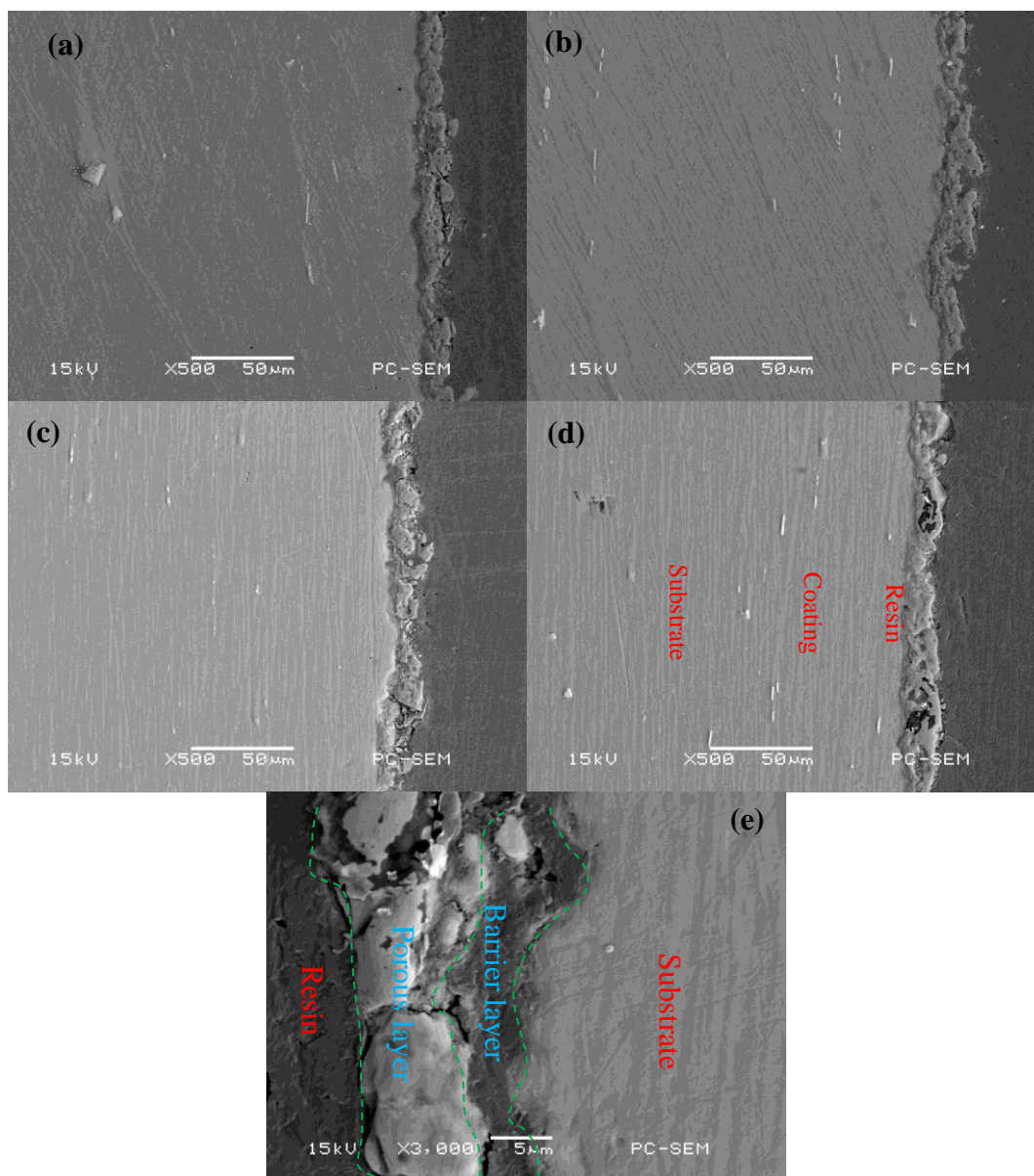


Figure 4. Cross-sectional morphology of PEO coatings with the treatment time: (a) 10 min, (b) 20 min, (c) 30 min, (d) 40 min, respectively. (e) shows the enlarged image of the coating with the longest treatment time, which clearly showed the double-layered structure of the coating.

The cross-section images of PEO coatings formed in the K_2ZrF_6 -containing electrolyte are showed in Fig.4. After comparison, it can be concluded that the coating with the maximum treatment time was of the thickest thickness value. The coating thickness is 8.2, 14.1, 18.4, 21.5 μm with the treatment time of 10, 20, 30 and 40 min, respectively. The thickness of the coating increased with the increment of the treatment time which is corresponding to the results measured by the thickness gauge. On the other hand, it is clearly showed that the coating can be divided into two parts: the inner barrier layer and the outer porous layer (See Fig.4e) [17].

3.3. Composition analysis

3.3.1 XRD analysis

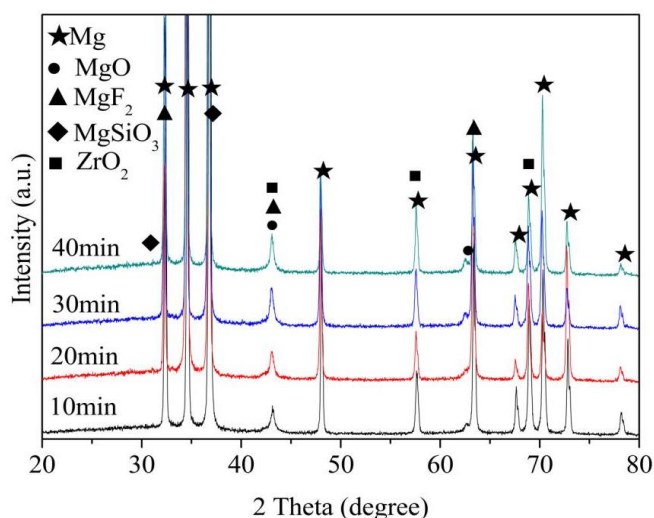
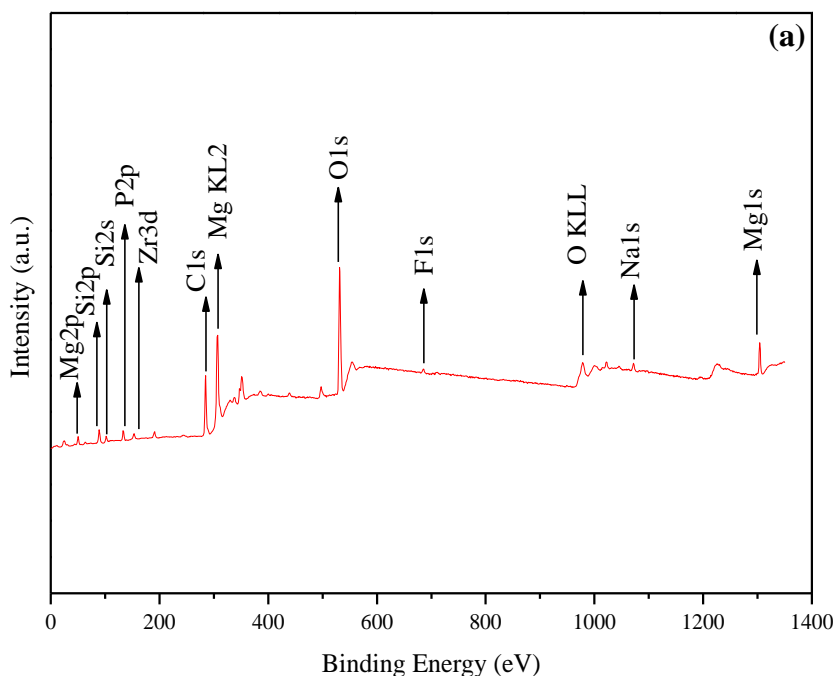


Figure 5. X-ray diffraction patterns of PEO coatings with the treatment time of 10, 20, 30 and 40 min.

The XRD patterns of the coatings fabricated in the electrolyte is presented in Fig.5. It is showed that the coating formed in such electrolyte was mainly composed of MgO, MgF₂, ZrO₂ and MgSiO₃. And, the content of ZrO₂ increased with the increasing treatment time. The formation of MgF₂ and ZrO₂ suggested that the additive K₂ZrF₆ was incorporated into the PEO reaction and formed the compounds. It should be noticed that some peaks corresponding to ZrO₂ is extremely high. This is because that the PEO coating is porous and the X-ray is easy to penetrate into the pores. So the Mg alloy was detected.

3.3.2 XPS analysis



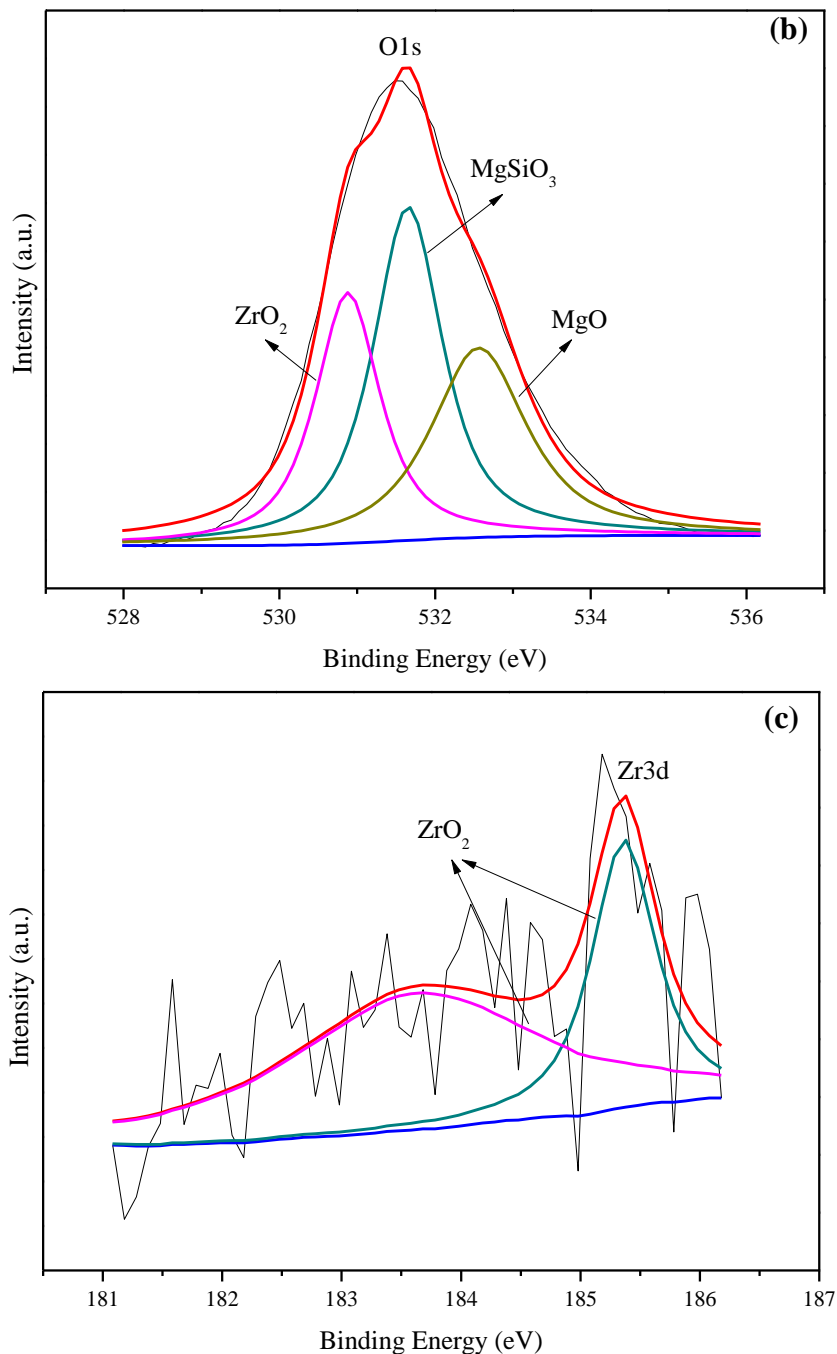


Figure 6. XPS spectra of PEO coatings with the treatment time of 40 min. (a) the survey spectrum, the specific spectra of (b) O1s, (c) Zr3d.

Fig.6 showed the XPS survey spectrum of PEO coating with 40 min treatment. After detection, it is indicated that the element of the coating was Mg, Si, O and Zr (See Fig.6a).

The photoelectron peaks of O1s and Zr3d are shown in Fig.6b and c, respectively (See Fig.6b and c). The O1s peak at 531.5 eV, can be decomposed into three peaks at 529.6 eV, 531.7 eV and 532.1 eV, corresponding to ZrO_2 , Mg_2SiO_3 and MgO, respectively. The binding energy peaks located at 185.5 eV and 183.3 eV are attributed to spin orbit splitting of the Zr3d components ($Zr3d_{3/2}$ and $Zr3d_{5/2}$).

3.4. Corrosion analysis

3.4.1. OCP-time curves

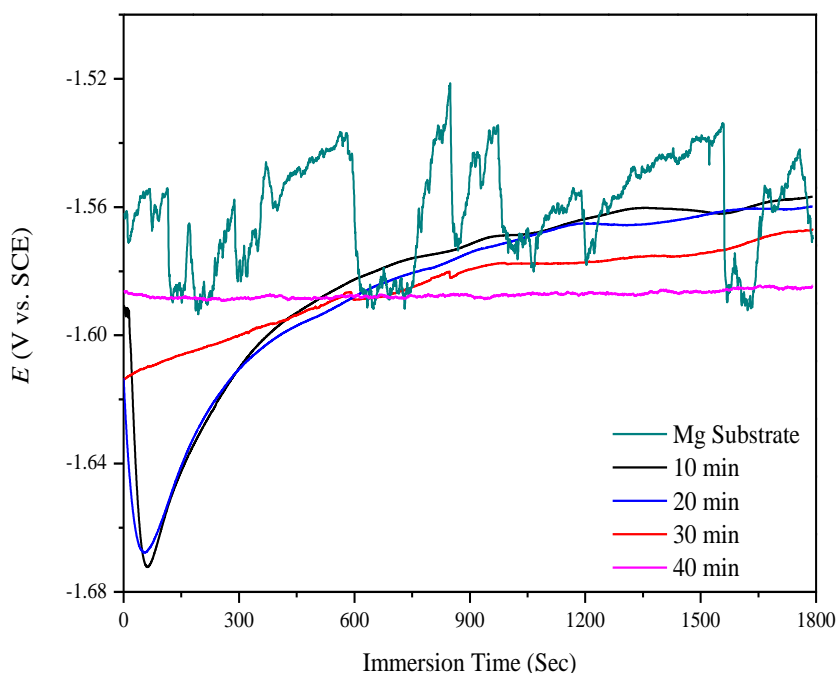


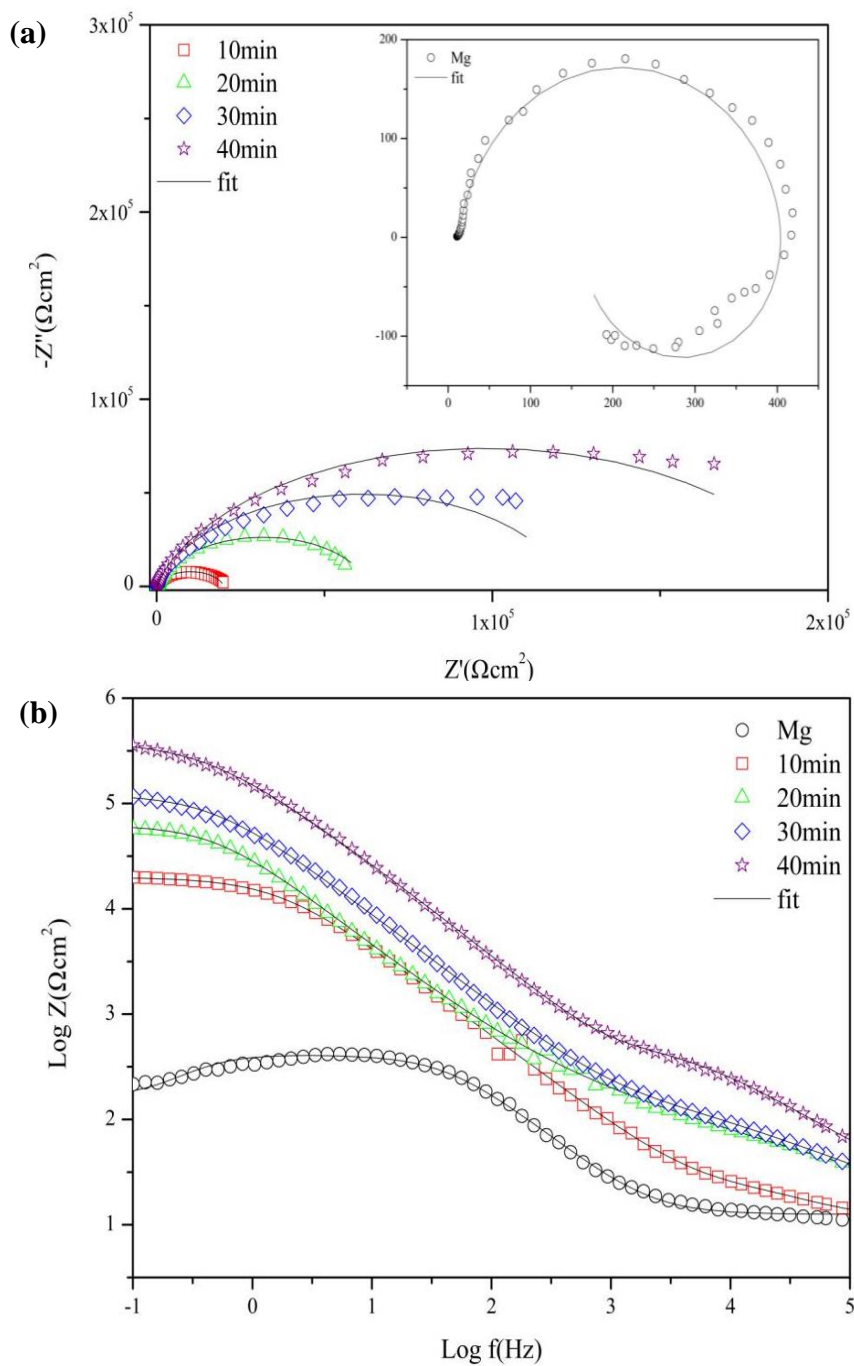
Figure 7. OCP-time curves of uncoated and PEO coated specimens formed in the electrolyte with 10, 20, 30 and 40 min.

Fig.7 presents the OCP-time curves of the uncoated AZ31 Mg alloy and PEO coatings in 3.5 wt.% NaCl aqueous solution. It is showed that the OCP of the Mg alloy substrate fluctuates with the immersion time during the whole test process. The OCP of the Mg alloy ranges from -1.52 mV vs. SCE to -1.60 mV vs. SCE. In general, the OCP of the Mg alloy decreased with the immersion time, which is owing to the dissolution of the very thin film (e.g. MgO or other Mg oxide) on the substrate and the active effect of the substrate. On the contrary, the OCP of the PEO coatings fluctuates at first and lasts for a few period and eventually becomes stable. It is suggested that the micro-pores on the PEO coatings were blocked by the corrosion products [18]. It should be point out that the OCP of the PEO coating formed in the electrolyte with 40 min treatment was stable during the whole immersion process, indicating that the coating possessed a higher stability in this corrosive environment.

3.4.2. EIS measurement

The uncoated and PEO coated AZ31 Mg alloys was studied by EIS test in 3.5 wt% NaCl aqueous solution to investigated their corrosion behavior. Fig.8 shows the EIS (Nyquist and Bode) plots. The magnified Nyquist plot of uncoated AZ31 Mg alloy (on the upper right of Fig.8a), indicated that the uncoated AZ31 Mg substrate is composed of a capacitive loop in high frequency range with an inductive loop in the low frequency range, which is similar to the previous reports [19]. Based on the previous reports [20], the chemical reaction of Mg alloy and the salt solution led to the appearance of capacitive

loop, which resulted in the Mg dissolution accompanied by the indicative of pitting corrosion. Besides, the Nyquist plot of PEO coatings showed the greater radius of the capacitive loop among them. Generally, the radius of the capacitive loop reflects the corrosion resistance of the coatings. That is, the bigger radius the capacitive loop is, the lower corrosion rate the coatings are.



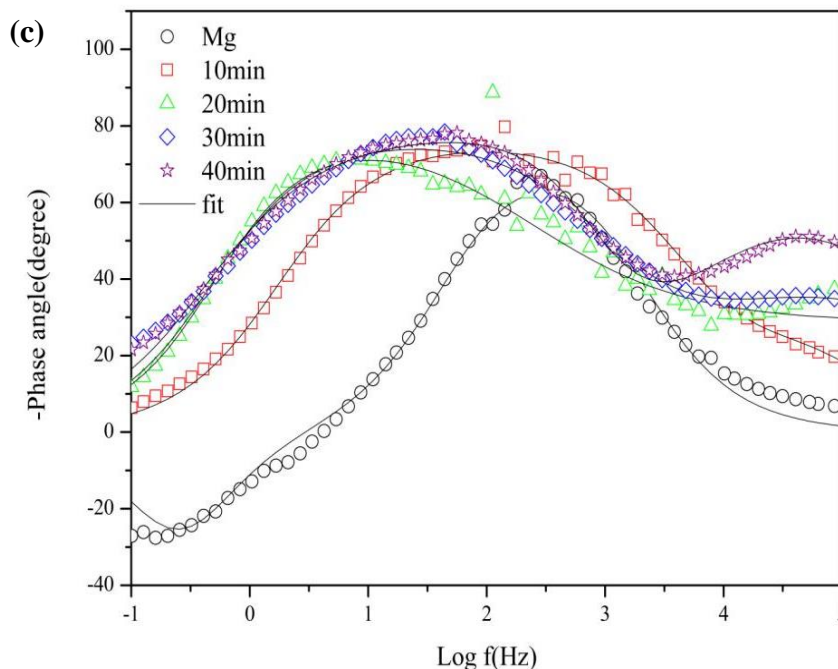


Figure 8. (a) Nyquist and (b), (c) Bode plots of uncoated and PEO coated AZ31 Mg alloy substrate in 3.5 wt% NaCl solution. Consequent lines correspond to fit using equivalent circuits of Fig.9 and symbols correspond to experimental values.

Apparently, the PEO coating with 40 min time was of the maximum capacitive loop. This directly showed that the coating obtained in the electrolyte after 40 min treatment showed the best corrosion resistance. The Nyquist plot (See Fig.8a) showed that the diameter of the the capacitive loop of the coatings increased with the increasing treatment time. Fig.8b shows that the impedance of the uncoated AZ31 Mg alloy ranged form 10^0 to $10^{2.5} \Omega\text{cm}^2$ approximately. This results is comparable to the previous study [21]. However, the impedance of PEO coatings was above $10^{5.5}$ at lower frequencies (See Fig.8b). This demonstrates that the PEO coatings with longer treatment time conspicuously enhanced the corrosion resistance of the AZ31 Mg alloy. To fit the EIS results, two time constants are required. The Bode phase angel plot in Fig.8c intuitively illustrates the results and consistent well with the feature of the Nyquist plots in Fig.8a. In the low frequency range, it can be seen that the phase angles of bare alloy is less than 0° (See Fig.8c). Such phenomena indicates that the pitting corrosion occurs.

The equivalent circuit model presented in Fig.9 was used to analyze the EIS results. A constant phase element (CPE) [22] which is represented by symbol Q was used which was used to instead a rigid capacitive element. The capacity element is illustrated as following:

$$Z_Q = \frac{1}{Y_0} (j\omega)^{-n} \tag{2}$$

In the formula, j is an imaginary unit ($j^2 = -1$) and ω is angular frequency ($\omega = 2\pi f$). The coefficient Y_0 or n ($-1 \leq n \leq 1$) is the parameter of CPE.

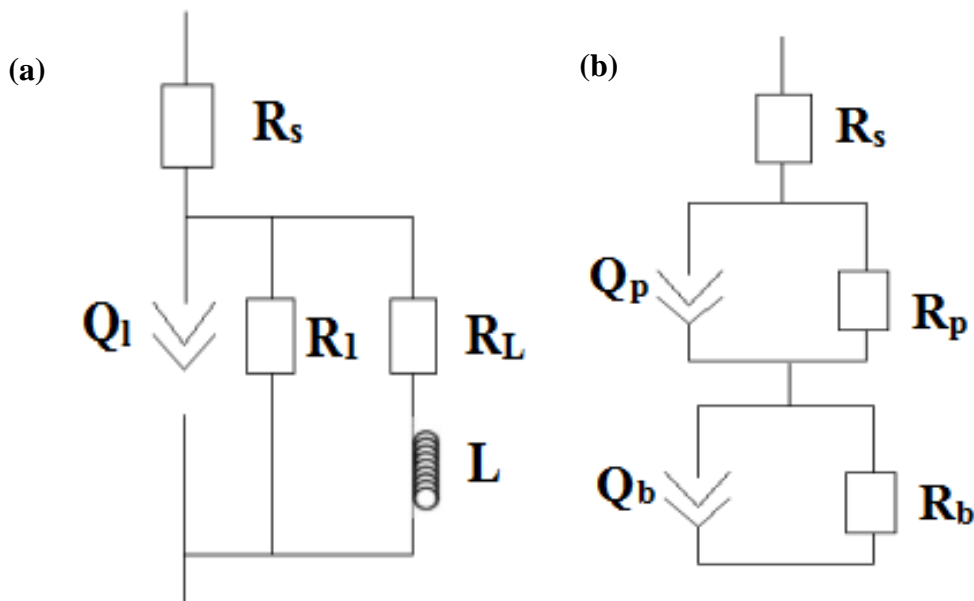


Figure 9. Equivalent circuits of the EIS plots for (a) uncoated and (b) PEO coated AZ31 Mg alloy in 3.5 wt% NaCl solution.

In the equivalent circuits (EC), R_s is the electrolyte resistance, R_L is the charge transfer resistance of pitting corrosion with the inductance L . R_p and R_b is the resistance of the outer porous and inner barrier layer, respectively (See Fig.9b). It should be pointed that as the uncoated AZ31 Mg alloy has no dense layer, the best fit EC is Fig.9a (See Fig.9a). In the figure, the fitted capacitance loop in high-frequency capacitance loop is defined by Q_l and R_l , which described the loose outer layer in the uncoated AZ31 Mg alloy (See Fig.9a). The onset of pitting corrosion reflected by the EC is described by R_L and L in the low-frequency inductive loop.

Table 3. Equivalent circuit data of (a) uncoated and PEO coatings with the treatment time: (b) 10, (c) 20, (d) 30 and (e) 40 min, respectively.

| Sample | R_s (Ω cm ²) | Q_l (Ω^{-1} s ⁿ cm ⁻²) | n_l | R_l (k Ω cm ²) | L (Ω^{-1} s ⁿ cm ⁻²) | R_L (k Ω cm ²) | |
|--------|------------------------------------|---|-------|-------------------------------------|---|-------------------------------------|-------------------------------------|
| (a) | 12.55 | 1.52×10^{-5} | 0.91 | 0.39 | 255 | 0.24 | |
| Sample | R_s (Ω cm ²) | Q_p (Ω^{-1} s ⁿ cm ⁻²) | n_p | R_p (k Ω cm ²) | Q_b (Ω^{-1} s ⁿ cm ⁻²) | n_b | R_b (k Ω cm ²) |
| (b) | 10.66 | 2.87×10^{-6} | 0.92 | 8.8 | 2.73×10^{-6} | 0.81 | 42.9 |
| (c) | 8.26 | 2.34×10^{-7} | 0.94 | 13.6 | 3.15×10^{-6} | 0.83 | 73.5 |
| (d) | 6.34 | 4.58×10^{-6} | 0.83 | 18.2 | 6.21×10^{-7} | 0.74 | 104.7 |
| (e) | 7.68 | 3.31×10^{-6} | 0.81 | 24.3 | 2.27×10^{-7} | 0.69 | 197.1 |

According to the equivalent circuits above (See Fig.9), EIS curves were best fitted, and the corresponding equivalent circuit parameters were listed in Table 3. Generally, the resistance value intuitively reflect the corrosion resistance of the coatings. That is, the higher the resistance value is, the better the corrosion resistance is. In the table, it is clearly showed that the PEO coatings was of low capacitance (CPE_p and CPE_b) and relatively high resistance (R_p and R_b). These evidences strongly

indicated that the coatings are able to protect the Mg alloy substrate, especially for the PEO coatings with the highest treatment time, which was of the highest R_p and R_b value than that of the other coatings. Besides, it is showed that the resistance value, i.e., the R_p and R_b value of PEO coatings, increased with the treatment time lasted. Which means that the corrosion resistance of the coatings increased with the treatment time increased from 10 min to 40 min.

3.4.3. Corrosion morphology

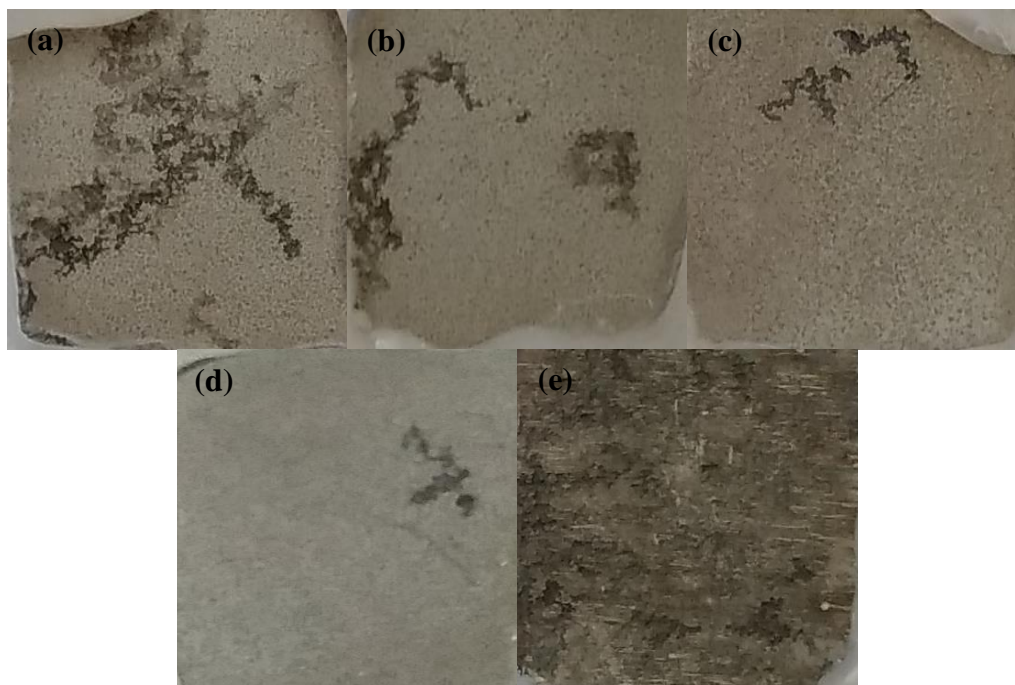


Figure 10. The appearance of specimens after long time salt solution immersion test in 3.5 wt% NaCl solution for 140 h: PEO coatings with treatment time of (a) 10, (b) 20, (c) 30, (d) 40 min and (e) AZ31B Mg alloy.

Fig.10 shows the images of uncoated and PEO coatings after 140 h immersion in 3.5 wt% NaCl solution. It is showed that the Mg substrate was almost completely covered by the black corrosion products (See Fig.10e). Nevertheless, the morphology of the PEO coatings are much better. The corrosion area of PEO coatings with the treatment time of 10, 20, 30, 40 min and Mg substrate are about 27%, 18%, 8%, 3% and 98% respectively. The observation of the corroded specimens is in good agreement with the electrochemical analysis results.

4. CONCLUSION

(1) The PEO coatings were fabricated in silicate-phosphate based electrolyte with the addition of K_2ZrF_6 . PEO coatings formed in the electrolyte were mainly composed of MgO, MgF_2 , ZrO_2 and $MgSiO_3$.

(2) The large fluctuations were observed in the OCP measurement in 30 min, while the PEO coatings first wave and eventually becomes stable. The PEO coating with 40 min treatment time of was registered as stable during the whole 30 min immersion time.

(3) The corrosion resistance of PEO coatings elevated with the treatment time increased, and the coating with the treatment time of 40 min showed the most superior corrosion resistance.

ACKNOWLEDGMENTS

This work is supported by the Natural Science Foundation of the Jiangsu Higher Education Institutions of China (Grant Nos. 19KJB430024), the Science Foundation of the Jiangsu Industrial Software Engineering Research Center (ZK190401) and the National Key Research and Development Program of China (Grant Nos. 2016YFB0300400).

References

1. Y.L. Song, Y.H. Liu, S.R. Yu, X.Y. Zhu and Q. Wang, *Appl. Surf. Sci.*, 254 (2008) 3014.
2. A. Ghasemi, V.S. Raja, C. Blawert, W. Dietzel and K.U. Kainer, *Surf. Coat. Technol.*, 202 (2008) 3513.
3. G. Song, A. Atrens and M. Dargusch, *Corros. Sci.*, 41 (1999) 249.
4. Q.P. Tran, T.S. Chin, Y.C. Kuo, C.X. Jin, T.Trung, C.V. Tuan and D.Q. Dang, *J. Alloys. Comp.*, 30 (2018) 289.
5. Z. Yang, R.Q. Wang, C. Liu, Y.K. Wu, D.D. Wang, X.T. Liu, X.Z. Zhang, G.R. Wu and D.J. Shen, *J. Mater. Eng. Perform.*, 28 (2019) 3652.
6. M.S. Naeini, M.Ghorbani and E. Chambari, *Metall. Mater. Trans. A*, 50 (2019) 3310.
7. S. Ahmadnia, S. Aliasghari and M. Ghorbani, *J. Mater. Eng. Perform.*, 28 (2019) 4120.
8. S. Stojadinović and R. Vasilić, *J. Lumin.*, 199 (2018) 240.
9. A.B. Khiabani, S. Rahimi, B. Yarmand, M. Mozafari, *Mater. Today*, 5 (2018) 15603.
10. T.S. Lim, H.S. Ryu and S.H. Hong, *Corr Sci.*, 62 (2012) 104.
11. H. Fadaee and M. Javidi, *J. Alloys Comp.*, 604 (2014) 36.
12. Y. Zhang, Y. Chen, X.Y. Duan, W.Q. Zheng and Y.W. Zhao, *Mater. Res. Express.*, 6 (2019) 126416.
13. X.P. Lu, S.P. Sah, N. Scharnagl, M. Störmer, M. Starykevich, M. Mohedano, C. Blawert, M.L. Zheludkevich, K.U. Kainer, *Surf. Coat. Technol.*, 269 (2015) 155.
14. J.J. Zhuang, Y.Q. Guo, N. Xiang, Y. Xiong, Q. Hu, R.G. Song, *Appl. Surf. Technol.*, 357 (2015) 1463.
15. J.L. Delplancke and R. Winand, *Electrochim. Acta*, 33 (1988) 1551.
16. S. Stojadinovic, R. Vasilic, M. Petkovic, B. Kasalica, I. Belca, A. Zekic and L.J.Zekovic, *Appl. Surf. Sci.*, 265 (2013) 226.
17. N. Xiang, R.G. Song, C. Wang, Q.Z. Mao, Y.J. Ge and J.H. Ding, *Corr. Eng. Sci. Technol.*, 51 (2016) 146.
18. S. Shen, Y. Zuo and X. Zhao, *Corros. Sci.*, 76 (2013) 275.
19. R. Gao, Q. Liu, J. Wang, X. Zhang, W. Yang, J. Liu and L. Liu, *Chem. Eng. J.*, 241 (2014) 352.
20. G. Song, A. Atrens, D.S. John, X. Wu and J. Nairn, *Corros. Sci.*, 39 (1997) 1981.
21. X.J. Cui, X.Z. Lin, C.H. Liu, R.S. Yang, X.W. Zheng and M. Gong, *Corros. Sci.*, 90 (2015) 402.
22. P. Su, X. Wu, Y. Guo and Z.H. Jiang, *J. Alloys Comp.*, 475 (2009) 773.